Science Advances
AAAS

advances.sciencemag.org/cgi/content/full/5/11/eaax5078/DC1

Supplementary Materials for

Discovery of fossil asteroidal ice in primitive meteorite Acfer 094

Megumi Matsumoto*, Akira Tsuchiyama, Aiko Nakato, Junya Matsuno, Akira Miyake, Akimasa Kataoka, Motoo Ito, Naotaka Tomioka, Yu Kodama, Kentaro Uesugi, Akihisa Takeuchi, Tsukasa Nakano, Epifanio Vaccaro

*Corresponding author. Email: m_matsumto@tohoku.ac.jp

Published 20 November 2019, *Sci. Adv.* **5**, eaax5078 (2019)
DOI: 10.1126/sciadv.aax5078

This PDF file includes:

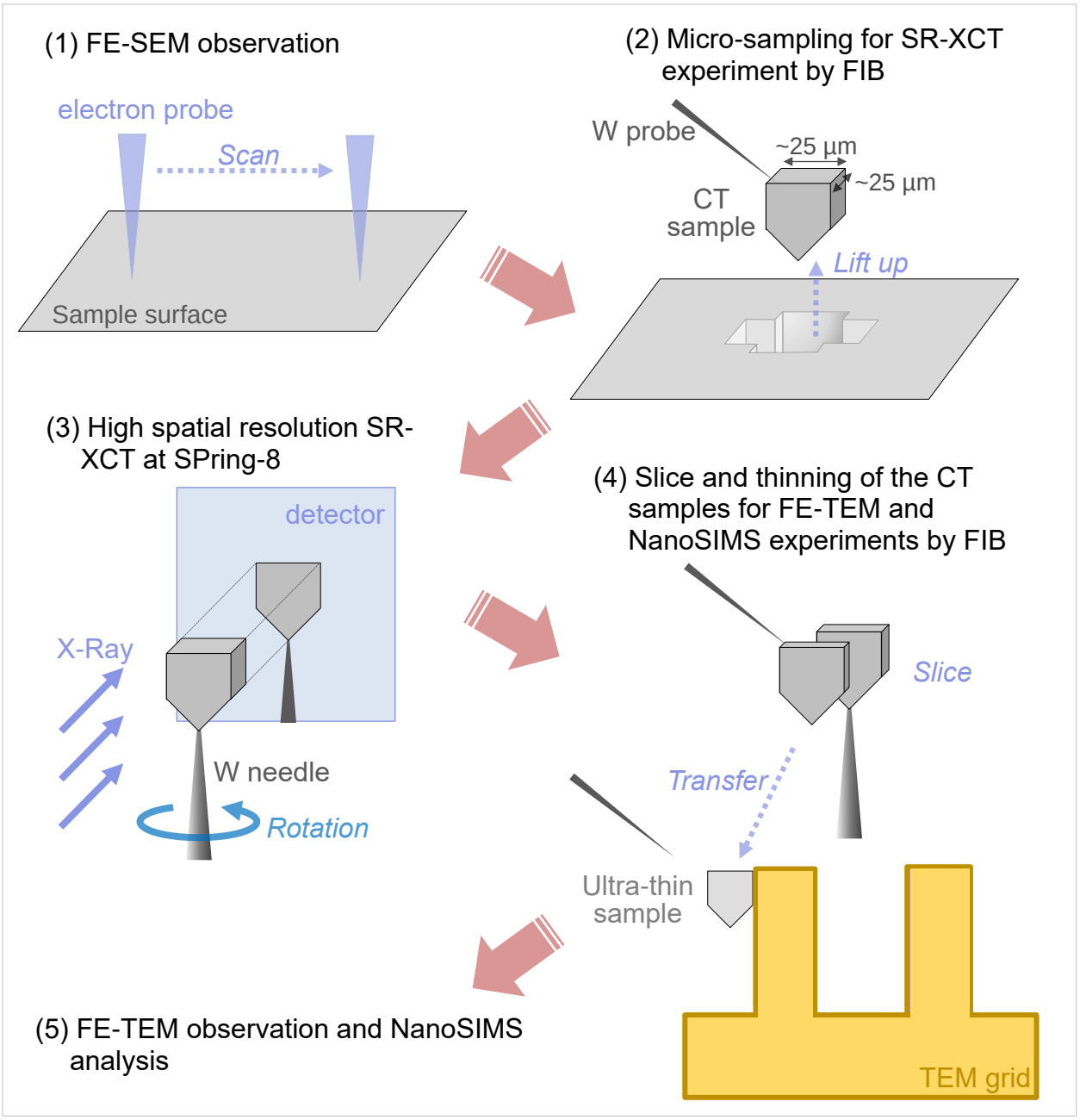

Fig. S1. Schematic illustration of the analytical protocol in this study.

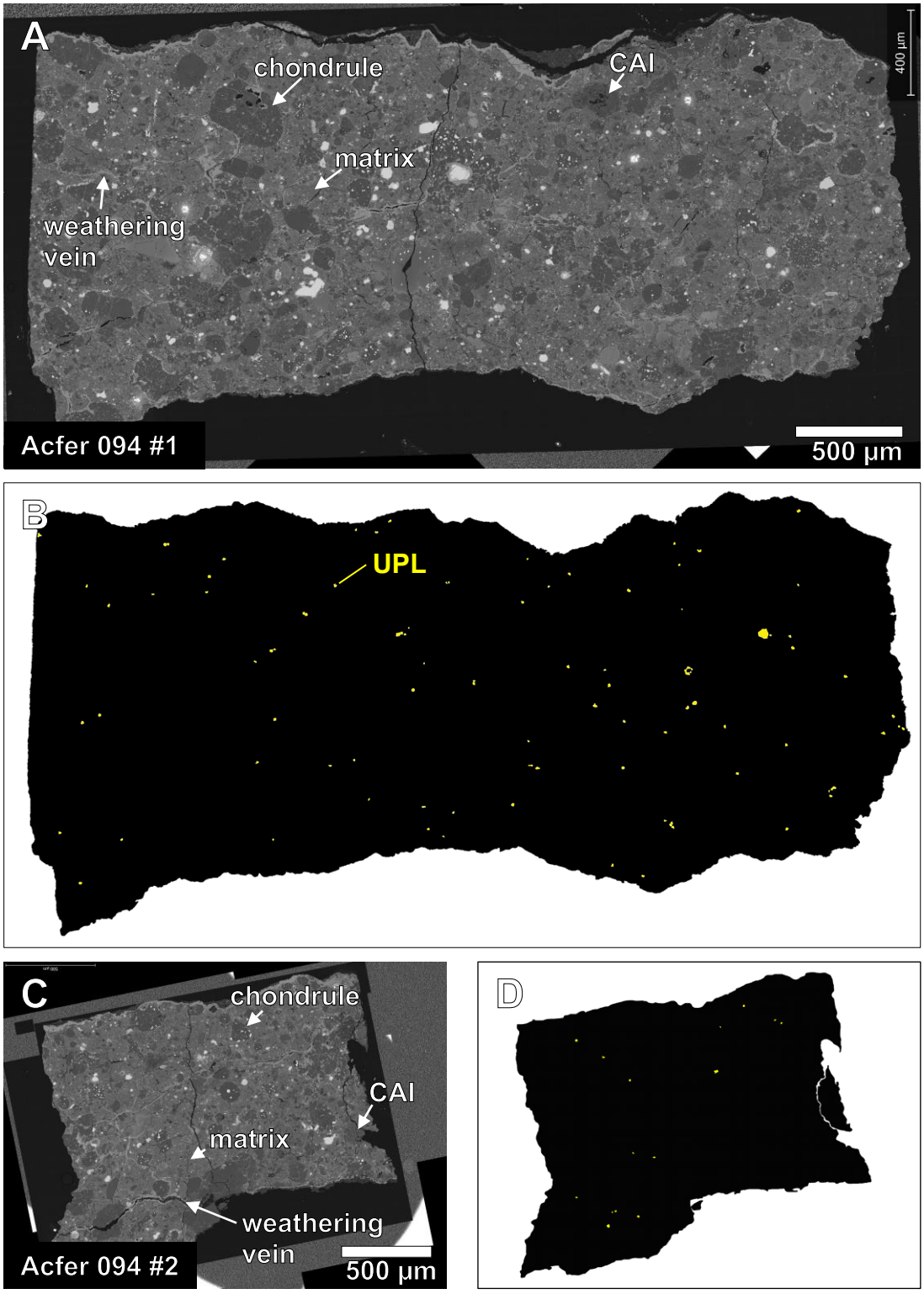

Fig. S2. SEM images of the two Acfer 094 polished sections, #1 and #2. BSE images of sections #1 and #2 (A and C) and their illustrations (B and D) show that UPLs (colored in yellow) are widely distributed in the polished sections.

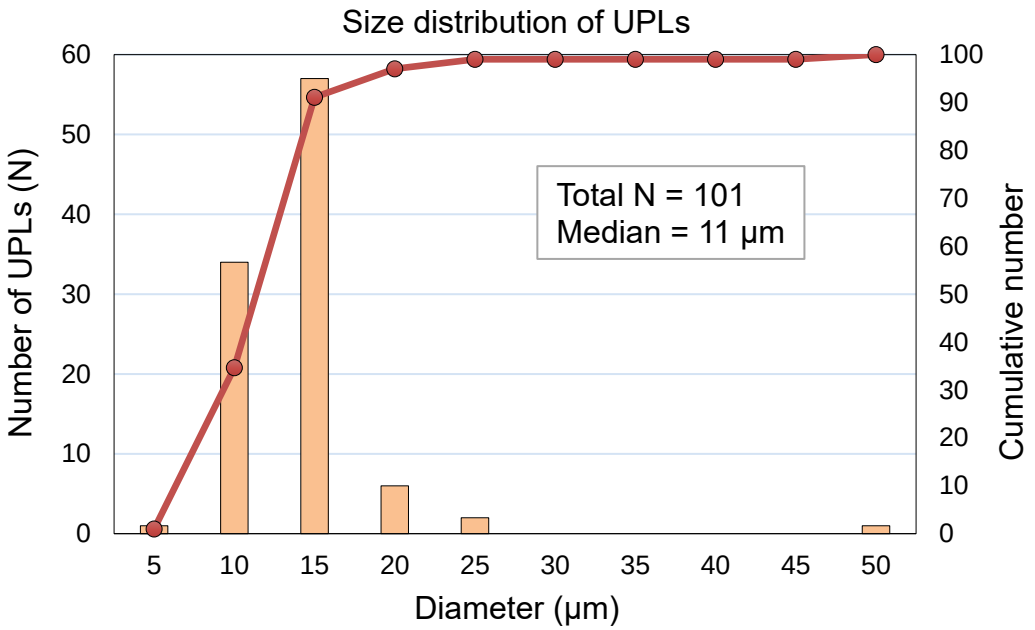

Fig. S3. Histogram showing the size distribution of UPLs. Most of them are <25 μm in diameter (sphere-equivalent diameter obtained from the cross-sectional area of individual UPL), with a median diameter of 11 μm. The cumulative count distribution is also shown.

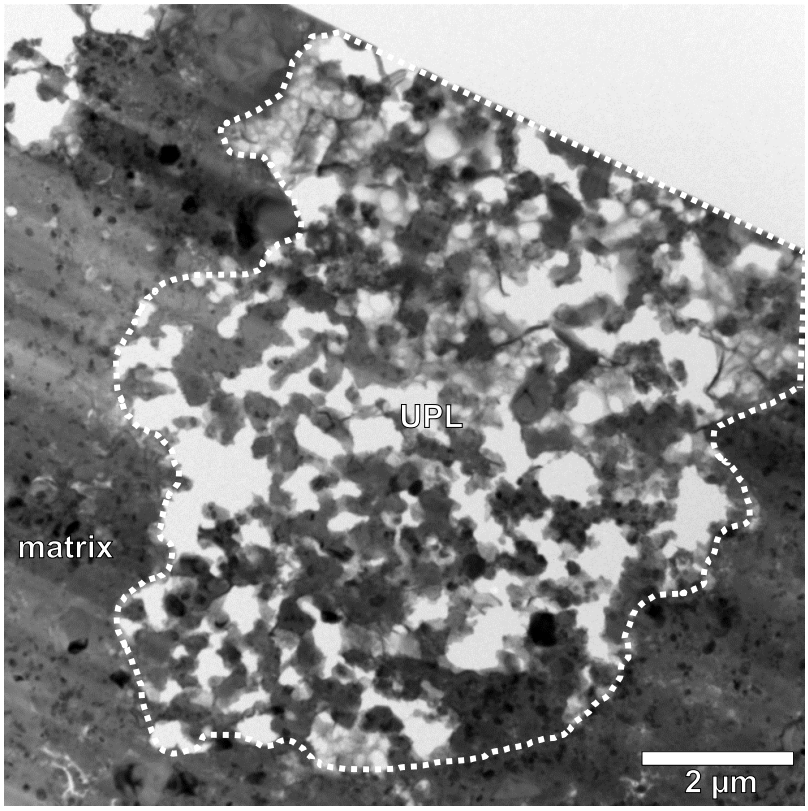

Fig. S4. BF-TEM image of a UPL. The bright regions correspond to pores. The UPL shows a highly porous texture compared to the surrounding matrix.

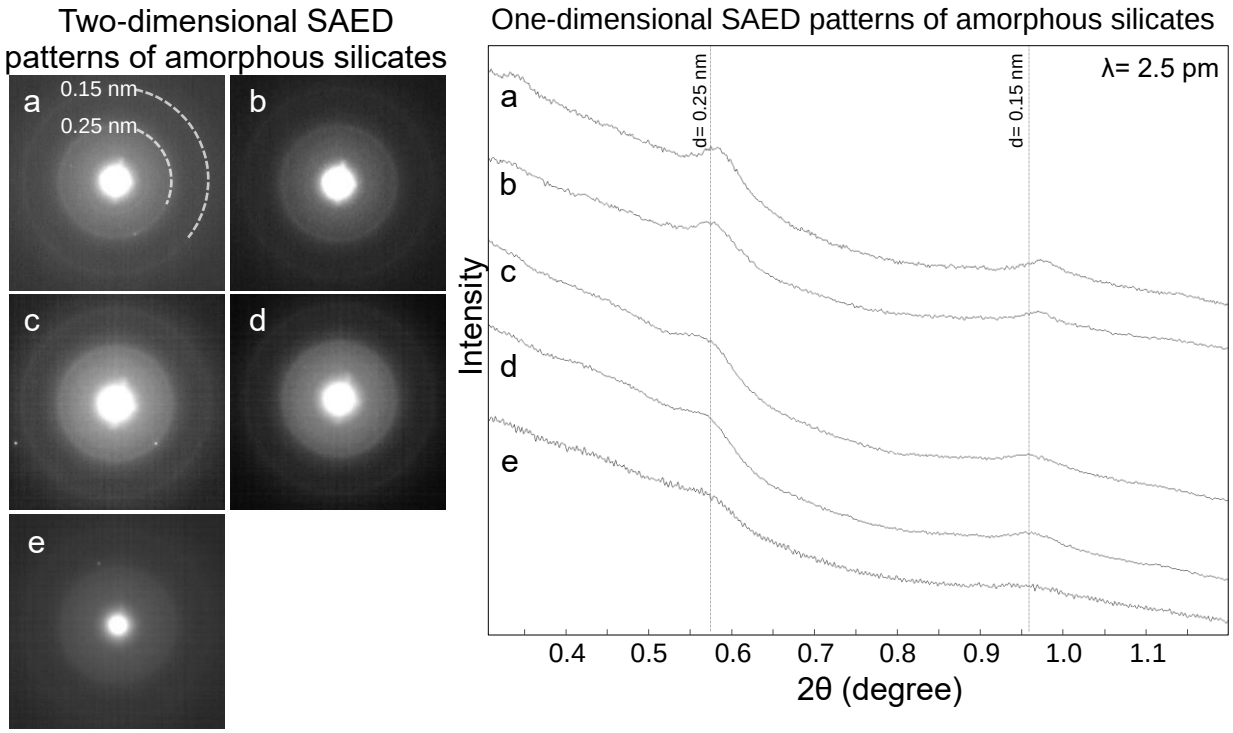

Fig. S5. SAED patterns of amorphous silicates in UPLs and in the matrix. The left panel shows the 2D SAED patterns of the five representative amorphous silicates (a–e). The right panel shows the 1D-converted SAED patterns of the same amorphous silicates (a–e). The SAED patterns of (a–d) contain weak rings with *d*-spacings of ~0.25 and ~0.15 nm, suggesting poorly crystallized states. The SAED pattern of (e) does not contain any such ring corresponding to amorphous materials.

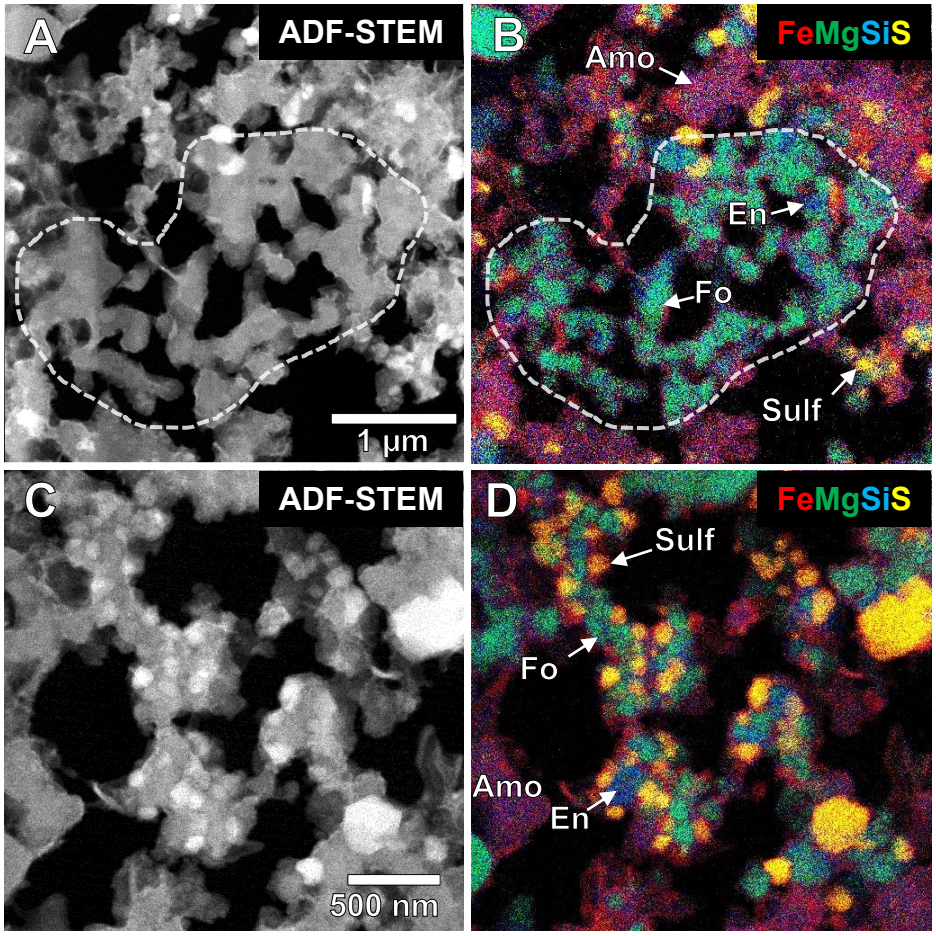

Fig. S6. STEM-EDS maps of equilibrated aggregate–like objects in UPL. An annular dark field (ADF) STEM image (A) and a combined STEM-EDS map (Fe in red, Mg in green, Si in blue, and S in yellow) (B) of an aggregate of forsterite (Fo; light green) and enstatite (En; cyan) show similarities to Type II EA in CP-IDPs *(2)*. Also shown are an ADF-STEM image (C) and a combined STEM-EDS map (again Fe in red, Mg in green, Si in blue, and S in yellow) (D) of an aggregate of forsterite, enstatite, and Fe–Ni sulfides (Sulf; yellow), showing similarities to Type I EA in CP-IDPs *(2)*. Amo: amorphous silicate.

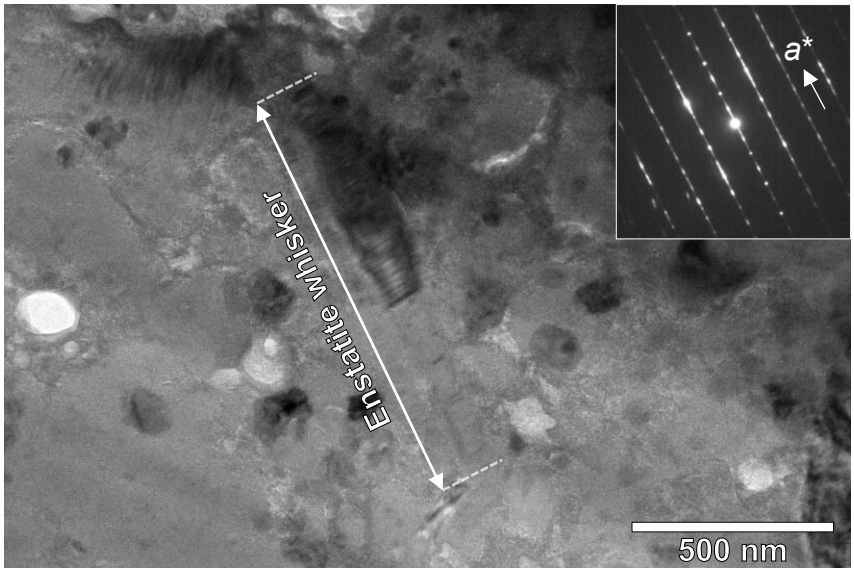

Fig. S7. BF-TEM image and SAED pattern of an enstatite whisker in the matrix. The enstatite whisker is elongated along the crystallographic *a*-axis.

Table S1. Compositions of GEMS-like materials in UPLs and in the matrix.

	UPL		UPL		UPL		matrix		matrix		matrix	
	wt.%	2σ	wt.%	2σ	wt.%	2σ	wt.%	2σ	wt.%	2σ	wt.%	2σ
O	40.82	1.46	37.11	1.19	47.58	2.11	44.19	1.38	45.45	1.39	47.24	1.34
Mg	5.59	0.56	4.92	0.40	4.37	0.78	11.60	0.75	8.66	0.65	4.36	0.43
Al	1.86	0.30	n.d.	n.d.	n.d.	n.d.	1.13	0.21	1.20	0.22	3.24	0.34
Si	16.77	0.91	11.60	0.58	13.69	1.28	16.82	0.86	16.75	0.86	16.09	0.80
S	n.d.	n.d.	6.05	0.39	n.d.	n.d.	n.d.	n.d.	n.d.	n.d.	0.91	0.18
Ca	2.17	0.32	1.19	0.17	n.d.	n.d.	1.69	0.27	1.56	0.26	2.57	0.31
Fe	32.79	1.32	36.87	1.07	34.36	2.03	24.58	1.12	26.39	1.16	25.59	1.10
Ni	n.d.	n.d.	2.25	0.29	n.d.	n.d.	n.d.	n.d.	n.d.	n.d.	n.d.	n.d.
H_2O*	3.0–3.4		9.2–9.6		17.6–18.0		6.9–7.1		9.7–10.0		14.1–14.4	

*Values calculated under the assumption that S and Ni are derived from sulfides and using the value of $Fe^{3+}/\Sigma Fe = 0.66–0.73$ *(34)* for iron oxidation state.

Table S2. Brief summary of textural and mineralogical characteristics of UPL, CP-IDP, and UPL-like lithology in the Paris meteorite.

	UPL in Acfer 094	UPL-like lithology in Paris*[1]	CP-IDP*[2]
Texture	highly porous	porous	highly porous
(porosity in %)	(~40%)	(no data)	(>50%)
Mineralogy	amorphous silicate, forsterite, enstatite (including whisker), Fe–Ni sulfides, organics, poorly crystallized phyllosilicate	amorphous silicate, forsterite*[3], enstatite*[3], Fe–Ni sulfides, Fe oxide, organics, fine fibrous material	amorphous silicate, forsterite, enstatite (including whisker), Fe–Ni metal, Fe–Ni sulfides, organics
Characteristics of amorphous silicate	GEMS-like texture without Fe–Ni metal, hydrated	GEMS-like texture without Fe–Ni metal, hydrated*[4]	GEMS, dry

*[1]Data from *(8)*. *[2]Data from *(1–4)*. *[3]Presence of Mg-rich silicate whisker was presented in *(8)*.
*[4]Exact water contents were not presented in *(8)*.

Table S3. Oxygen isotopic compositions of UPL and matrix.

	$\delta^{17}O$	$\delta^{18}O$
GEMS-like materials#1	−9.3 ± 25.0	16.1 ± 9.4
GEMS-like materials#2	−6.64 ± 4.52	15.24 ± 2.03
Organics#1	8.18 ± 23.80	31.49 ± 9.69
Organics#2	25.4 ±12.7	30.4 ± 8.7
UPL/matrix mean	4.0 ± 9.0	29.8 ± 4.8
GEMS in CP-IDP mean *(2)*	−16.1 ± 12.5	−2.3 ± 4.00
Acfer 094 bulk meteorite *(15)*	−3.91	1.17

*Errors are 1σ. $^{17}O/^{16}O_{smow}$ = 0.0003829, $^{18}O/^{16}O_{smow}$ = 0.0020052.